ORIGINAL PAPER

Heat capacity of γ-Fe$_2$SiO$_4$ between 5 and 303 K and derived thermodynamic properties

Wenjun Yong · E. Dachs · A. C. Withers · E. J. Essene

Abstract A multi-anvil device was used to synthesize 24 mg of pure γ-Fe$_2$SiO$_4$ crystals at 8.5 GPa and 1,273 K. The low-temperature heat capacity (C_p) of γ-Fe$_2$SiO$_4$ was measured between 5 and 303 K using the heat capacity option of a physical properties measurement system. The measured heat capacity data show a broad λ-transition at 11.8 K. The difference in the C_p between fayalite and γ-Fe$_2$SiO$_4$ is reduced as the temperature increases in the range of 50–300 K. The gap in C_p data between 300 and 350 K of γ-Fe$_2$SiO$_4$ is an impediment to calculation of a precise C_p equation above 298 K that can be used for phase equilibrium calculations at high temperatures and high pressures. The C_p and entropy of γ-Fe$_2$SiO$_4$ at standard temperature and pressure ($S°_{298}$) are 131.1 ± 0.6 and 140.2 ± 0.4 J mol^{-1} K^{-1}, respectively. The Gibbs free energy at standard pressure and temperature ($\Delta G°_{f,298}$) is calculated to be –1,369.3 ± 2.7 J mol^{-1} based on the new entropy data. The phase boundary for the fayalite–γ-Fe$_2$SiO$_4$ transition at 298 K based on current thermodynamic data is located at 2.4 ± 0.6 GPa with a slope of 25.4 bars/K, consistent with extrapolated results of previous experimental studies.

W. Yong (✉) · E. J. Essene
Department of Geological Sciences, University of Michigan,
Ann Arbor, MI 48109-1005, USA
e-mail: wenjuny@umich.edu

E. Dachs
Fachbereich Materialwissenschaften, Universität Salzburg,
Hellbrunnerstr. 34, 5020 Salzburg, Austria

A. C. Withers
Department of Geology and Geophysics,
University of Minnesota, Minneapolis, MN 55455, USA

Introduction

Calorimetric measurements of the heat capacity (C_p) of many high-pressure phases are incomplete. The entropy value is critical to thermodynamic calculations of the phase equilibrium relations, and the most precise way to obtain the entropy value is by measuring the heat capacity as a function of temperature. However, high-pressure phases must be synthesized experimentally in a multi-anvil device, and the minimum amount of sample needed for low-temperature heat capacity measurement by conventional low-temperature adiabatic calorimetry (low-TAC, e.g., Robie and Hemingway 1972), which is 10–30 g in general, would take hundreds of experimental runs just to make enough sample, hence prohibiting the heat capacity measurement in practice. Recently, the heat capacity option of the Physical Properties Measurement System (PPMS, produced by Quantum Design®), based on heat-pulse calorimetry, has been shown to give precise low-temperature heat capacity measurements of milligram-sized samples (e.g., Dachs and Bertoldi 2005; Yong et al. 2006).

Fayalite (Fe$_2$SiO$_4$) is one end-member of olivine, the most abundant mineral in the earth's upper mantle. Numerous experimental studies on Fe$_2$SiO$_4$ have shown that fayalite transforms into a phase with a spinel structure (γ-Fe$_2$SiO$_4$) at pressures higher than 4–5 GPa at 700–1,300 K (e.g., Akimoto et al. 1965, 1967; Inoue 1975; Sung and Burns 1976; Furnish and Bassett

1983; Yagi et al. 1987). The natural occurrence of γ-Fe_2SiO_4 with Fe/(Fe + Mg) ratios ranging from 0.62 to 0.99 has also been reported in a shocked chondrite meteorite (Xie et al. 2002; Xie and Sharp 2004). The transition in $(Mg,Fe)_2SiO_4$ is regarded to play an important role in the formation of seismic discontinuities. Therefore, direct measurement of the thermodynamic properties of γ-Fe_2SiO_4 and fayalite is of great importance in terms of understanding geophysical applications at mantle conditions. Although the thermodynamic properties of fayalite have been well characterized, those of γ-Fe_2SiO_4 are still in need of characterization. The enthalpy and high-temperature heat capacity of γ-Fe_2SiO_4 were measured by Akaogi et al. (1989) and Watanabe (1982), respectively. However, for the aforementioned reason, the low-temperature heat capacity and thus entropy value of γ-Fe_2SiO_4 was not determined calorimetrically. In this study, the heat capacity data of γ-Fe_2SiO_4 were measured between 5 and 303 K using the PPMS machine at Salzburg, and the entropy and Gibbs free energy at standard temperature and pressure (STP) were calculated from the measured heat capacity data.

Experimental procedures

Sample synthesis and characterization

Fayalite was synthesized from a stoichiometric mixture of Fe_3O_4 and SiO_2. After mixing in an agate pestle and mortar, the starting material was reacted at 1,200°C for 48 h in a CO–CO_2 gas stream, adjusted to buffer oxygen fugacity at a value of two log units below fayalite–magnetite–quartz equilibrium. A 3-mm diameter Au capsule was loaded with more than 30 mg of fayalite powder and sealed by welding. The γ-Fe_2SiO_4 used in this study was synthesized from pure fayalite starting material in a 1,000-ton Walker-type multi-anvil device at the University of Minnesota. The experimental assemblage consisted of tungsten carbide anvils with 12 mm truncations, a cast MgO–Al_2O_3–SiO_2–Cr_2O_3 octahedron, straight-walled graphite heater and internal MgO spacers. The temperature was controlled using a $W_3Re_{97}/W_{25}Re_{75}$ thermocouple, which was located on top of the Au capsule with a 0.35-mm disk of MgO extrusion for electrical isolation. The sample was pressurized to 8.5 GPa before heating at 1,273 K for 12 h. The experiment was quenched by turning off the power to the heater and then slowly depressurized to ambient pressure. The run product was examined by powder X-ray diffraction and electron microprobe

(EMP) analysis, and single phase γ-Fe_2SiO_4 was confirmed.

Heat capacity measurement

The molar heat capacity at constant pressure (C_p) of γ-Fe_2SiO_4 in the temperature range of 5–303 K was measured at 1 atm using the heat capacity option of the PPMS at Salzburg University in Austria. A powdered sample of γ-Fe_2SiO_4 (24.0 mg) was sealed into a small Al pan with a lid and placed on a 4 mm × 4 mm wide sapphire platform that has a thermometer and a heater attached to the lower side. The C_p data were first collected at 60 different temperatures from 5 to 303 K with a logarithmic spacing, and three measurements were performed at each temperature. More C_p data were collected around 12 K and from 50 to 303 K with a linear spacing in a second run. A brief summary of this technique is given by Yong et al. (2006), and a more detailed description including discussions of the precision and accuracy of the C_p measurement by PPMS is in Lashley et al. (2003) and Dachs and Bertoldi (2005).

Results and discussion

The measured molar heat capacity (C_p) data of γ-Fe_2SiO_4 are listed in Table 1 and plotted in Fig. 1. A C_p polynomial of the general form $C_p = k_0 + k_1T^{-0.5} + k_2T^{-2} + k_3T^{-3} + k_4T + k_5T^2 + k_6T^3$ was used to fit the measured molar C_p data, which were split into several temperature regions due to the λ-anomaly. The C_p data below 5 K were estimated from a plot of C_p/T versus T^2 and a linear extrapolation to 0 K. The entropy of γ-Fe_2SiO_4 at STP is calculated from analytical and stepwise integration of the smoothed C_p data and was found to be identical within error when calculated by numerical integration. The resulting entropy value is 140.2 ± 0.4 J mol^{-1} K^{-1} (error is two standard deviations). The uncertainty in the entropy is estimated as described by Dachs and Geiger (2006).

In comparison with the C_p data of fayalite (Fig. 2, triangles), which has a very sharp λ-transition at 64.9 K as well as a small rounded hump near 16 K (Robie et al. 1982), the C_p data of γ-Fe_2SiO_4 (Fig. 2, circles) exhibit a broad maximum (λ-transition) at 11.8 K and a weak shoulder around 7 K, possibly related to a Schottky-anomaly (e.g., Gopal 1966) arising from the Fe^{2+} 3d orbitals. The broad λ-transition is likely due to a paramagnetic–antiferromagnetic transition just as the 65 K transition in fayalite (Santoro et al. 1966;

Table 1 Measured heat capacity data of γ-Fe$_2$SiO$_4$

T (K)	C_p (J mol^{-1} K^{-1})	T (K)	C_p (J mol^{-1} K^{-1})	T (K)	C_p (J mol^{-1} K^{-1})	T (K)	C_p (J mol^{-1} K^{-1})
5.14	1.863	49.98	17.48	12.05	13.181	143.42	72.03
5.14	1.856	50.03	17.53	12.06	13.192	143.43	71.97
5.14	1.852	53.56	18.97	12.06	13.204	148.5	74.54
5.51	2.289	53.56	18.96	12.27	13.072	148.57	74.81
5.51	2.286	53.62	19.04	12.28	13.064	148.57	74.88
5.9	2.855	57.41	20.83	12.29	13.059	153.6	77.38
5.9	2.865	57.41	20.84	12.5	12.897	153.68	77.28
5.91	2.885	57.47	20.87	12.51	12.893	153.69	77.34
6.32	3.588	61.53	22.98	12.51	12.889	158.8	79.71
6.32	3.591	61.53	22.95	12.73	12.7	158.88	79.78
6.32	3.621	61.61	22.93	12.74	12.702	158.88	79.71
6.77	4.424	65.95	25.41	12.74	12.7	163.96	82.21
6.77	4.421	65.97	25.36	12.96	12.5	164.04	82.15
6.77	4.458	66.04	25.54	12.97	12.497	164.05	82.27
7.22	5.248	70.7	28.14	12.97	12.489	169.06	84.59
7.22	5.253	70.71	28.12	13.19	12.288	169.14	84.61
7.22	5.284	70.79	28.28	13.19	12.287	169.14	84.6
7.74	6.144	75.78	31.31	13.19	12.292	174.27	87.38
7.74	6.117	75.78	31.27	13.41	12.09	174.35	87.3
7.74	6.112	75.85	31.24	13.42	12.087	174.36	87.44
8.29	7.005	81.16	35.01	13.42	12.086	179.37	89.43
8.29	6.987	81.16	35.07	13.64	11.905	179.45	89.55
8.29	6.992	81.24	35.12	13.65	11.896	179.45	89.36
8.88	7.936	86.98	38.55	13.65	11.893	184.57	91.87
8.88	7.917	86.98	38.58	13.87	11.716	184.66	91.95
8.88	7.927	87.07	38.58	13.88	11.713	184.66	91.65
9.52	8.988	93.21	42.28	13.88	11.714	189.74	93.76
9.52	8.994	93.22	42.17	14.1	11.564	189.82	93.51
9.52	9.014	93.31	42.41	14.11	11.56	189.82	93.63
10.2	10.339	99.92	46.81	14.11	11.565	194.9	96.38
10.2	10.342	99.92	46.67	14.32	11.436	194.98	96.22
10.2	10.356	100.01	46.7	14.33	11.439	194.99	96.01
10.93	12.135	107.09	50.98	14.33	11.438	200.06	98.49
10.94	12.138	107.09	50.84	14.55	11.314	200.14	98.32
10.94	12.143	107.19	50.98	14.56	11.326	200.15	98.25
11.7	13.176	114.79	56.07	14.56	11.321	205.22	100.45
11.71	13.208	114.79	55.81	14.77	11.234	205.3	100.17
11.71	13.211	114.88	56.21	14.78	11.24	205.3	100.11
12.53	12.869	123.03	60.83	14.79	11.238	210.36	101.73
12.55	12.863	123.03	60.86	15	11.151	210.45	101.72
12.55	12.87	123.13	60.94	15.01	11.16	210.47	101.89
13.42	12.084	131.88	65.61	15.01	11.157	215.52	103.82
13.44	12.077	131.88	65.53	15.22	11.04	215.62	103.91
13.44	12.077	131.97	65.78	15.22	11.059	215.62	103.89
14.38	11.408	141.36	70.9	15.23	11.071	220.62	105.6
14.4	11.411	141.36	71.03	50.53	17.65	220.7	105.63
14.4	11.411	141.45	71.81	50.6	17.74	220.71	105.86
15.42	11.082	151.51	76.47	50.6	17.73	225.83	107.59
15.43	11.081	151.51	76.37	55.67	19.85	225.92	107.43
15.43	11.086	151.61	76.34	55.76	19.99	225.93	107.64
16.53	11.009	162.4	81.91	55.76	19.99	230.91	109.16
16.53	11.014	162.41	81.85	60.83	22.43	231	109.39
16.53	11.018	162.49	81.75	60.92	22.62	231.01	109.54
17.71	11.076	174.08	87.7	60.93	22.56	236.14	111.7
17.71	11.082	174.08	87.68	66	25.28	236.23	111.76
17.71	11.077	174.15	87.83	66.09	25.48	236.24	111.92
18.97	11.167	186.65	94.28	66.09	25.47	241.31	113.72
18.98	11.17	186.65	94.25	71.16	28.26	241.39	114.19
18.98	11.17	186.72	94.25	71.25	28.6	241.4	114
20.34	11.294	200.04	100.1	71.25	28.45	246.45	115.75
20.34	11.291	200.04	100.19	76.31	31.21	246.54	116.3
		200.09	100.2	76.4	31.81	246.55	116.13

Table 1 continued

T (K)	C_p (J mol^{-1} K^{-1})	T (K)	C_p (J mol^{-1} K^{-1})	T (K)	C_p (J mol^{-1} K^{-1})	T (K)	C_p (J mol^{-1} K^{-1})
20.34	11.297	214.38	105.7	76.4	31.89	251.61	117.74
21.79	11.413	214.38	105.74	81.46	35.16	251.69	118.14
21.79	11.421	214.41	105.57	81.55	35.22	251.7	117.85
21.8	11.414	229.76	110.36	81.56	35.1	256.67	118.97
23.35	11.552	229.76	110.34	86.58	38.29	256.75	119.2
23.35	11.552	229.77	110.23	86.66	38.43	256.77	119.24
23.36	11.542	246.24	116.64	86.67	38.29	261.89	120.81
25.02	11.742	246.27	116.49	91.75	41.3	261.98	121.45
25.02	11.734	246.28	116.48	91.84	41.49	262.07	121.55
25.04	11.732	263.81	121.38	91.85	41.55	267.06	122.98
26.81	11.91	263.92	121.3	96.91	44.59	267.13	122.98
26.81	11.898	263.94	121.04	97	44.71	267.15	123.31
26.83	11.959	282.7	126.59	97	44.83	272.11	124.38
28.73	12.07	282.85	126.47	102.07	48.1	272.19	124.05
28.73	12.064	282.85	126.58	102.16	47.88	272.21	124.15
28.75	12.086	302.95	132.51	102.16	48.12	277.36	125.07
30.78	12.293	303.14	132.3	107.22	50.93	277.43	125.24
30.78	12.296	303.15	132.52	107.31	51.29	277.44	125.24
30.81	12.311			107.32	51.15	282.51	126.28
32.99	12.642			112.35	54.25	282.57	126.65
32.99	12.644	10.68	11.502	112.43	54.54	282.59	126.69
33.02	12.664	10.69	11.492	112.44	54.41	287.56	128.03
35.35	13.09	10.69	11.491	117.51	57.51	287.62	128.05
35.35	13.089	10.91	12.091	117.59	57.7	287.64	128.34
35.39	13.121	10.92	12.104	117.6	57.84	292.8	129.95
37.89	13.739	10.92	12.102	122.7	60.65	292.88	130.2
37.89	13.728	11.14	12.582	122.78	60.73	292.88	129.94
37.92	13.756	11.14	12.593	122.79	60.86	297.95	131.21
40.6	14.33	11.14	12.589	127.86	63.53	298.02	131.15
40.6	14.326	11.37	12.946	127.94	63.61	298.03	131.38
40.64	14.364	11.37	12.944	127.95	63.86	302.99	132.38
43.51	15.14	11.37	12.959	133.02	66.05	303.06	132.46
43.51	15.14	11.59	13.145	133.1	66.23	303.06	132.6
43.56	15.18	11.6	13.165	133.1	66.22		
46.63	16.2	11.6	13.152	138.14	69.07		
46.63	16.2	11.82	13.228	138.22	69.16		
46.68	16.25	11.83	13.233	138.22	69.02		
49.98	17.45	11.83	13.234	143.34	71.84		

Ehrenberg and Fuess 1993). The C_p of γ-Fe$_2$SiO$_4$ measured by PPMS is generally lower than that of fayalite (Robie et al. 1982) in the temperature range of 50–300 K (Fig. 2). However, the difference of C_p between the two polymorphs decreases with increasing temperature. As a result, the C_p data of γ-Fe$_2$SiO$_4$ and fayalite differ less than 1 J mol^{-1} K^{-1} at 300 K. If this trend continues to high temperatures, the entropy difference (ΔS) and enthalpy difference (ΔH) for the fayalite–γ-Fe$_2$SiO$_4$ transition will approach constant values, which means the only cause that can change the slope of the transition boundary will be a difference in volume. However, this situation is not supported by the C_p data of fayalite and γ-Fe$_2$SiO$_4$ measured between 350 and 700 K by Watanabe (1982), who showed there is a 4–6 J mol^{-1} K^{-1} difference between the C_p values of these two phases in the range of 350–700 K. Unfortunately, the C_p of γ-Fe$_2$SiO$_4$ between 300 and

350 K has not yet been measured and the PPMS routinely measures the C_p data only in the range 2–303 K. Therefore a reasonable and precise fitting of C_p polynomial above 298 K cannot be undertaken until the discrepancy between the available DSC data and the result of this study is resolved. Until then, an accurate representation of the phase boundary for the fayalite–γ-Fe$_2$SiO$_4$ transition at high pressures and temperatures is cumbersome.

The entropy of γ-Fe$_2$SiO$_4$ at standard pressure and temperature (S°_{298}) calculated from integration of the C_p data in this study may be compared with estimates from previous studies. The available estimates of the S°_{298} of γ-Fe$_2$SiO$_4$ range from 134 to 146 J mol^{-1} K^{-1} (e.g., Fei and Saxena 1986; Fei et al. 1991; Fabrichnaya 1998; Jacobs et al. 2001; Jacobs and de Jong 2005). The S°_{298} value of γ-Fe$_2$SiO$_4$ calculated from the measured C_p data in this study, 140.2 ± 0.4 J mol^{-1} K^{-1}, in the
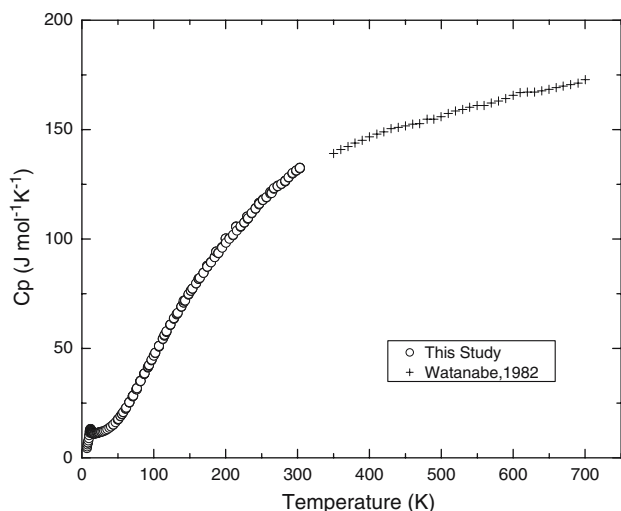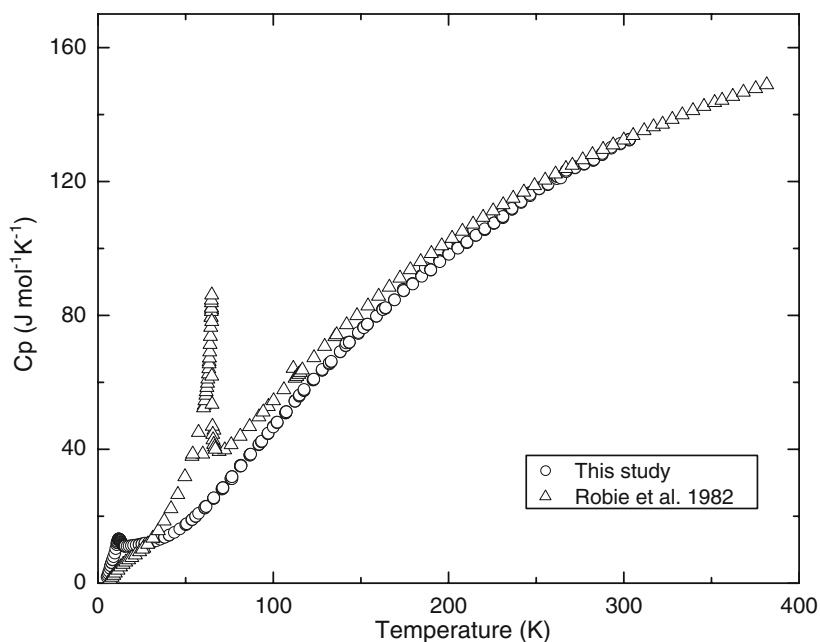
Fig. 1 Comparison of the heat capacity data of γ-Fe$_2$SiO$_4$ measured by PPMS (*circles*) with those measured by DSC (*crosses*)

midpoint of the range of estimates, will serve as a strong constraint and substantial improvement for the thermodynamic data base of the Fe$_2$SiO$_4$ system. The enthalpy of the fayalite–γ-Fe$_2$SiO$_4$ transition at standard pressure and temperature ($\Delta H^{\circ}_{tr,298}$) is given by Akaogi et al. (1989) as 6.6 ± 2.4 kJ mol^{-1}. The enthalpy of formation at 298 K ($\Delta H^{\circ}_{f,298}$) of fayalite from elements is given by Robie and Hemingway (1995) as $-1,478.2 \pm 1.3$ kJ mol^{-1}. By combining these two studies, the $\Delta H^{\circ}_{f,298}$ of γ-Fe$_2$SiO$_4$ is calculated to be $-1,471.6 \pm 2.7$ kJ mol^{-1}, which together with our new entropy value, results in the value of Gibbs free

energy at standard pressure and temperature ($\Delta G^{\circ}_{f,298}$), $-1,369.3 \pm 2.7$ kJ mol^{-1}.

The fayalite–γ-Fe$_2$SiO$_4$ transition boundary at 298 K can be calculated using the equation defined as follows:

$$\Delta G(P, 298) = \Delta H^{\circ}_{tr,298} - 298.15 \Delta S^{\circ}_{tr,298}$$
$$+ \int_0^P \Delta V(P', 298) \mathrm{d}P' = 0 \qquad (1)$$

where $\Delta H^{\circ}_{tr,298}$ and $\Delta S^{\circ}_{tr,298}$ are enthalpy and entropy changes, respectively, for the fayalite–γ-Fe$_2$SiO$_4$ transition at STP, and $\Delta V(P, 298)$ is the volume change at pressure P and at 298 K. The pressure dependence of the molar volume was expressed by the Birch–Murnaghan equation of state:

$$P = \frac{3}{2} K_0 \left[\left(\frac{V^{\circ}}{V} \right)^{7/3} - \left(\frac{V^{\circ}}{V} \right)^{5/3} \right]$$
$$\times \left\{ 1 - \frac{3}{4} \left(4 - K'_0 \right) \left[\left(\frac{V^{\circ}}{V} \right)^{2/3} - 1 \right] \right\} \qquad (2)$$

where K_0 and K'_0 are the isothermal bulk modulus and its pressure derivative, respectively. The fayalite–γ-Fe$_2$SiO$_4$ transition at 298 K is calculated to be at 2.4 ± 0.6 GPa based on current thermodynamic data given in Table 2. The error of the calculated pressure mainly results from the uncertainties of measured enthalpy change of the transition (Akaogi et al. 1989), with a small contribution from the uncertainties of measured entropies of fayalite and γ-Fe$_2$SiO$_4$ by Robie et al. (1982) and this study, respectively.

Fig. 2 Comparison of heat capacity data of γ-Fe$_2$SiO$_4$ (*circles*) with fayalite (*triangles*)

Table 2 Thermodynamic properties used for phase boundary calculation

Phase	$\mathring{H}_{f,298}$ (kJ mol^{-1})	$\mathring{S}_{298}$ (J mol^{-1} K^{-1})	$\mathring{V}_{298}$ (cm^3 mol^{-1})	K_0 (GPa)	K'_0	$\alpha = a + bT + cT^{-2}$ (K^{-1})[a]		
						$a \times 10^5$	$b \times 10^9$	$c \times 10$
Fayalite	$-1{,}478.2 \pm 1.3$[b]	151 ± 0.2[c]	46.28[d]	134[e]	4[f]	2.66	8.736	-2.487
γ-Fe$_2$SiO$_4$	$-1{,}471.6 \pm 2.7$[g]	140.2 ± 0.4[h]	42.04[i]	197[j]	4[f]	2.455	3.591	-3.703

[a] Fei and Saxena (1986)

[b] Robie and Hemingway (1995)

[c] Robie et al. (1982)

[d] Akimoto et al. (1976)

[e] Kudoh and Takeda (1986)

[f] Assumed

[g] Calculated from Akaogi et al. (1989)

[h] This study

[i] Marumo et al. (1977)

[j] Sato (1977)

The slope of the fayalite–γ-Fe$_2$SiO$_4$ transition at 298 K is also calculated using the Clausius–Clapeyron equation:

$$\frac{dP}{dT} = \frac{\Delta S(P, 298)}{\Delta V(P, 298)} \tag{3}$$

where the entropy values at high pressure are corrected with a second order approximation using thermal expansion data at 298 K (Table 2) in the following way:

$$S(P, 298) \simeq S°_{298} - \Delta P \alpha V°_{298} \tag{4}$$

Substituting $P = 2.4$ GPa into Eqs. 2–4, the slope of the fayalite–γ-Fe$_2$SiO$_4$ transition at 298 K is calculated to be 25.4 bars/K.

Experimental determinations of the fayalite–γ-Fe$_2$SiO$_4$ transition are plotted and extrapolated to 298 K for comparison with our calculated phase boundary location at 298 K in Fig. 3. Even though most of these experiments were undertaken at high temperatures, between 1,000 and 1,500 K, the extrapolated locations of the transition boundaries by Akimoto et al. (1967) and Yagi et al. (1987) at 298 K agree with our calculation within 0.4 GPa whereas the extrapolated position of the transition by Akimoto et al. (1977) lies at higher pressure. Moreover, the calculated slope of the fayalite–γ-Fe$_2$SiO$_4$ transition, 25.4 bars/K, is in excellent agreement with these experimental studies (Fig. 3), where the slope was given by either 25 bars/K (Akimoto et al. 1977; Yagi et al. 1987) or 26 bars/K (Akomoto et al. 1967). Because of the missing C_p data of γ-Fe$_2$SiO$_4$ between 300 and 350 K, a precise calculation of the phase
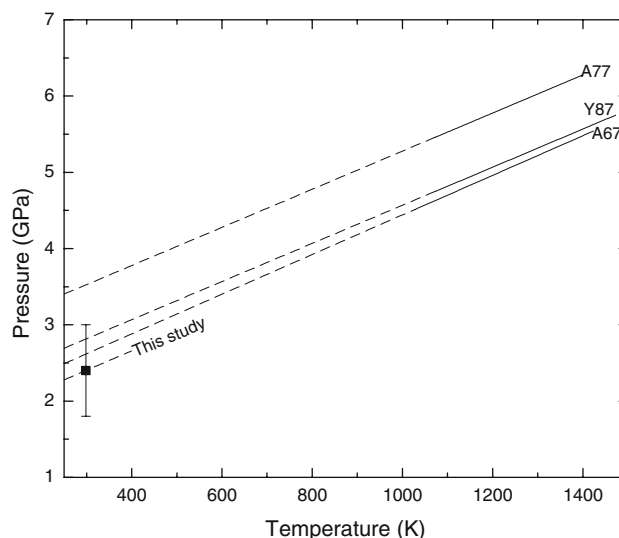

Fig. 3 Comparison of the phase transition boundary at 298 K calculated in this study with previous experimental studies. *Black square* represents our calculated location of phase transition boundary with two standard deviations. The calculated slope at 298 K is also plotted for comparison. *A67* Akimoto et al. (1967), *A77* Akimoto et al. (1977), *Y87* Yagi et al. (1987)

boundary above 298 K cannot be completed at present.

References

Akaogi M, Ito E, Navrotsky A (1989) Olivine-modified spinel–spinel transition in the system Mg_2SiO_4–Fe_2SiO_4: calorimetric measurements, thermochemical calculation, and geophysical application. J Geophys Res 94:15671–15685

Akimoto S, Fujisawa H, Katsura T (1965) Olivine–spinel transition in Fe_2SiO_4 and Ni_2SiO_4. J Geophys Res 66:1969–1977

Akimoto S, Komada E, Kushiro I (1967) Effect of pressure on the melting of olivine and spinel polymorphs of Fe_2SiO_4. J Geophys Res 68:679–686

Akimoto S, Matsui Y, Syono Y (1976) High-pressure crystal chemistry of orthosilicates and formation of the mantle transition zone. In: Strens RGJ (eds) The physics and chemistry of minerals and rocks. Wiley, New York, pp 327–363

Akimoto S, Yagi T, Inoue K (1977) High temperature–pressure phase boundaries in silicate systems using in situ X-ray diffraction. In: Manghnani MH, Akimoto S (eds) High-pressure research: application in geophysics. Academic, New York, pp 585–602

Dachs E, Bertoldi C (2005) Precision and accuracy of the heat-pulse calorimetric technique: low temperature heat capacities of milligram-sized synthetic mineral samples. Eur J Mineral 17:251–259

Dachs E, Geiger CA (2006) Heat capacities and entropies of mixing of pyrope–grossular ($Mg_3Al_2Si_3O_{12}$–$Ca_3Al_2Si_3O_{12}$) garnet solid solutions: a low-temperature calorimetric and a thermodynamic investigation. Am Mineral 91:8894–9006

Ehrenberg H, Fuess H (1993) Analytical interpretation and simulation of the static magnetic properties of synthetic α-Fe_2SiO_4. J Phys Condens Matter 5:3663–3672

Fabrichnaya O (1998) The assessment of thermodynamic parameters for solid phases in the Fe–Mg–O and Fe–Mg–Si–O systems. Calphad 22:85–125

Fei Y, Saxena SK (1986) A thermochemical data base for phase equilibria in the system Fe–Mg–Si–O at high pressure and temperature. Phys Chem Miner 13:311–324

Fei Y, Mao H, Mysen BO (1991) Experimental determination of element partitioning and calculation of phase relations in the MgO–FeO–SiO_2 system at high pressure and high temperature. J Geophys Res 96:2157–2169

Furnish MD, Bassett WA (1983) Investigation of the mechanism of the olivine–spinel transition in fayalite by synchrotron radiation. J Geophys Res 88:10333–10341

Gopal ESR (1966) Specific heats at low temperatures. Plenum, New York

Inoue K (1975) Development of high temperature and high pressure X-ray diffraction apparatus with energy dispersive technique and its geophysical applications. Ph.D. thesis, Tokyo University, Tokyo

Jacobs MHG, de Jong BHWS (2005) An investigation into thermodynamic consistency of data for the olivine, wadsleyite and ringwoodite form of $(Mg,Fe)_2SiO_4$. Geochim Cosmochim Acta 69:4361–4375

Jacobs MHG, de Jong BHWS, Oonk HAJ (2001) The Gibbs energy formulation of α, γ, and liquid Fe_2SiO_4 using Grover, Getting and Kennedy's empirical relation between volume and bulk modulus. Geochim Cosmochim Acta 65:4231–4242

Kudoh Y, Takeda H (1986) Single crystal X-ray diffraction study on the bond compressibility of fayalite, Fe_2SiO_4 and rutile, TiO_2 under high pressure. Physica B 139–140:333–336

Lashley JC, Hundley MF, Migliori A, Sarrao JL, Pagliuso PG, Darling TW, Jaime M, Cooley JC, Hults WL, Morales L, Thoma DJ, Smith JL, Boerio-Goates J, Woodfield BF, Stewart GR, Fisher RA, Phillips NE (2003) Critical examination of heat capacity measurements made on a quantum design physical property measurement system. Cryogenics 43:369–378

Marumo F, Isobe M, Akimoto S (1977) Electron-density distributions in crystals of γ-Fe_2SiO_4 and γ-Co_2SiO_4. Acta Crystallogr B 33:713–716

Robie RA, Hemingway BS (1972) Calorimeters for heat of solution and low-temperature heat capacity measurement. U.S. Geol Surv Prof Paper 755, 32 pp

Robie RA, Hemingway BS (1995) Thermodynamic properties of minerals and related substances at 298.15 K and 1 bar (10^5 Pascals) pressure and at higher temperatures. US Geol Surv Bull 2131:461

Robie RA, Finch CB, Hemingway BS (1982) Heat capacity and entropy of fayalite (Fe_2SiO_4) between 5.1 and 383 K: comparison of calorimetric and equilibrium values of the QFM buffer reaction. Am Mineral 67:463–469

Santoro RP, Newnham RE, Nomura S (1966) Magnetic properties of Mn_2SiO_4 and Fe_2SiO_4. J Phys Chem Solids 27:655–666

Sato Y (1977) Equation of state of mantle minerals determined through high-pressure X-ray study. In: Manghnani MH, Akimoto S (eds) High-pressure research: application in geophysics. Academic, New York, pp 307–323

Sung CM, Burns RG (1976) Kinetics of high-pressure phase transformations: implications to the evolution of the olivine–spinel transition in the downgoing lithosphere and its consequences on the dynamics of the mantle. Tectonophysics 31:1–32

Watanabe H (1982) Thermochemical properties of synthetic high-pressure compounds relevant to the earth's mantle. In: Manghnani MH, Akimoto S (eds) High-pressure research in geophysics. Center for Academic Publications, Japan, pp 441–464

Xie ZD, Sharp TG (2004) High-pressure phases in shock-induced melt veins of the Umbarger L6 chondrite: constraints of shock pressure. Meteorit Planet Sci 39:2043–2054

Xie ZD, Tomioka N, Sharp TG (2002) Natural occurrence of Fe_2SiO_4–spinel in the shocked Umbarger L6 chondrite. Am Mineral 87:1257–1260

Yagi T, Akaogi M, Shimomura O, Suzuki T, Akimoto S (1987) In situ observation of the olivine–spinel phase transition in Fe_2SiO_4 using synchrotron radiation. J Geophys Res 92:6207–6213

Yong W, Dachs E, Withers AC, Essene EJ (2006) Heat capacity and phase equilibria of hollandite polymorph of $KAlSi_3O_8$. Phys Chem Miner 33:167–177